

Angle-resolved ultraviolet photoelectron spectroscopy of the unoccupied band structure of graphite

T. Takahashi, H. Tokailin,* and T. Sagawa

Department of Physics, Tohoku University, Sendai 980, Japan

(Received 14 June 1985)

The energy dispersion of conduction (or unoccupied) bands of graphite has been studied by angle-resolved ultraviolet photoelectron spectroscopy. Photoemission peaks originating in the conduction bands were successfully separated from those of the valence bands by comparing two sets of angle-resolved ultraviolet photoelectron spectra excited by the He I and He II resonance lines. Three conduction bands were found in the energy range of 7–13 eV above the Fermi level and one of them showed a remarkable energy dispersion in the $\Gamma K H A$ plane in the Brillouin zone. The present experimental results have been compared with the results of earlier experiments using photoelectron, secondary-electron, electron-energy-loss, photoyield, and inverse photoelectron spectroscopies as well as with some theoretical calculations. The usefulness of angle-resolved (secondary) photoelectron spectroscopy to study unoccupied band structure has been demonstrated.

I. INTRODUCTION

The electronic structure of graphite has been intensively studied both theoretically and experimentally: however, it was only relatively recently that the overall valence-band structure was established experimentally by angle-resolved ultraviolet photoelectron spectroscopy (ARUPS).^{1–5} In contrast to the valence states, the structure of the conduction (or unoccupied) band is still controversial^{6,7} and a limited number of experimental studies^{8–14} have been performed. Recently Fauster *et al.*¹³ have succeeded in mapping out the lowest conduction band of graphite using angle-resolved inverse photoemission, which has proved to be very useful in studying the empty states of materials.

We have already presented preliminary results of the ARUPS study of graphite⁵ and discussed the valence-band structure by comparing these results with earlier experiments^{1–3} and some theoretical calculations.^{6,7,15,16} Photoelectron spectroscopy has been regarded as a powerful technique to study valence states of materials. However, it is well known that photoelectron spectra are largely modified by conduction or final states and sometimes conduction bands themselves appear as prominent structures in the photoelectron spectra.¹⁷ The photoemission peaks originating in conduction states are produced through inelastic scattering among electrons; a considerable portion of photoexcited electrons suffer energy losses during their transportation to the surface through several energy-loss mechanisms, electron-hole pair creation, plasmon loss, etc., and, as a result, these secondary electrons roll down through the conduction bands and pile up at the high density of the conduction states. If we perform angle-resolved energy analyses of these inelastically scattered electrons, we can get k -resolved information about conduction-band structure because these electrons must have the same energies and wave vectors parallel to the surface (k_{\parallel}) as they had in the conduction bands just before they were emitted into vacuum. We can map out energy dispersions of conduction bands with this

“angle-resolved secondary-photoelectron spectroscopy” (ARSPES). Thus, ARSPES can become a useful experimental technique to study empty states and is complementary to conventional ARUPS in which the main concerns are directed to elastically scattered electrons representing valence-band structures. In actual measurements, however, both elastically and inelastically scattered electrons overlap with each other in a photoelectron spectrum. The method of separating experimentally these two kinds of electrons has been already established; peaks having kinetic energies independent of exciting energies are due to conduction states while peaks moving in accordance with the exciting energy are attributed to valence states.¹⁷ One may notice that ARSPES is essentially the same as angle-resolved secondary-electron spectroscopy (ARSES),³ where the excitation is induced by electrons.

In this study, we used two exciting lights, He I (21.22 eV) and He II (40.8 eV), to distinguish the origin (conduction or valence states) of structures in photoelectron spectra. Comparing the experimental results obtained by these two different exciting photon energies, we found some conduction bands which show clear energy dispersions in the energy range of from 0 to about 7 eV above the vacuum level. The present experimental results are compared with early experiments using ARUPS,^{3,4} secondary-electron spectroscopy (SES),^{8,9} electron-energy-loss spectroscopy (EELS),¹⁴ and x-ray^{10,11} and ultraviolet^{12,13} inverse photoelectron spectroscopies as well as with some theoretical calculations.^{6,7}

II. EXPERIMENTAL

A synthesized single-crystalline graphite (Kish graphite) sample was supplied by Toshiba Ceramics Co. The preparation and purification procedures have been described elsewhere.¹⁸ The typical crystal size is about $2 \times 2 \times 0.2$ mm³. The Laue diffraction pattern of the sample showed that it is a good single crystal with almost no rotational disorder of layers as observed in highly-oriented

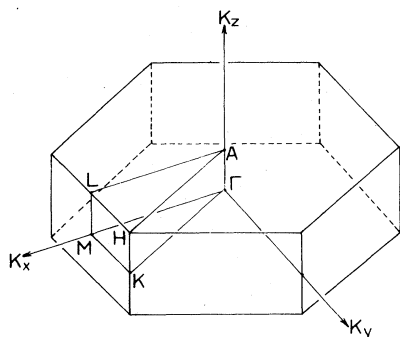


FIG. 1. Brillouin zone of graphite.

pyrolytic graphite (HOPG).

The ARUPS spectra were measured with the He I and He II resonance lines as exciting sources using a highly-angle-resolved ultraviolet photoelectron spectrometer constructed at our laboratory.¹⁹ The total energy resolutions were about 0.1 and 0.2 eV for the He I and He II measurements, respectively. The angular resolution was estimated to be less than 1.5°. This high angular resolving power of the spectrometer has been already demonstrated in our previous ARUPS works on black phosphorus²⁰ and rhombohedral arsenic.²¹ The base pressure of the spectrometer was about 2×10^{-10} Torr. Photons were incident at about 45° onto the surface of the sample (mixed *s* and *p* polarizations). The sample was cleaved *in vacuo* along the basal plane to obtain a clean surface for the photoemission measurements. The orientation of the sample relative to the electron-energy analyzer was determined roughly in advance by the Laue pattern and then precisely in the spectrometer by the azimuthal- and polar-angle dependence of the ARUPS spectra. The ARUPS measurements were performed for two planes of high symmetry in the Brillouin zone; the ΓKHA and ΓMLA planes (see Fig. 1). The work function of the sample was determined from the cutoff of the secondaries of photoemission spectra and is about 4.6 eV. The Fermi level of the sample was referred to that of a silver film deposited onto the sample surface. No noticeable effect of oxidation of the sample was detected during the measurements.

III. RESULTS AND DISCUSSION

Figures 2 and 3 show ARUPS spectra for the ΓKHA plane of graphite excited by He I and He II resonance lines. Typical peak count of spectra was 1000–2000. The present ARUPS spectra are far better resolved than those reported in earlier studies^{1,3} of graphite with the same He I and He II resonance lines; for example, a doublet structure of the first narrow peak just below the Fermi level in the He I spectrum for a polar angle of $\theta=55^\circ$ (Fig. 2), which corresponds to the doublet of π bands at the *K* point, is not well resolved in the earlier data.³ As for the He II measurement, the present spectrum for $\theta=0^\circ$ (Fig. 3) has a narrow leading peak at about 4 eV which relates to the highest σ band at the Γ point; this peak appears as a shoulder of the second peak at about 8 eV in the earlier

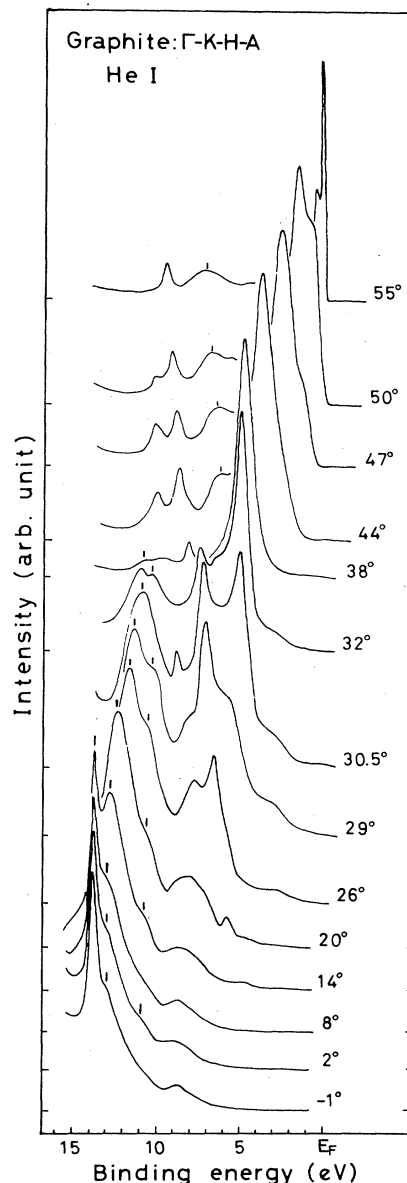


FIG. 2. Angle-resolved He I (21.22 eV) photoemission spectra of graphite measured for the ΓKHA plane. Polar angles referred to the surface normal are indicated on each spectrum. Peaks and shoulders denoted by tick marks originate in conduction bands.

measurement¹ (Fig. 1 in Ref. 1). These well-resolved features of the present ARUPS spectra are presumably due to the high angular resolution in this study and the good crystallinity of the synthesized Kish graphite.

As found in Figs. 2 and 3, photoemission spectral features differ considerably between the two sets of ARUPS spectra. These differences may be produced by the conduction states and are discussed in detail later. In the He II measurement (Fig. 3), π and σ valence bands of graphite are clearly identified in the spectra; the π band shows a doublet structure for a polar angle $\theta=0^\circ$ in the energy range of 8–10 eV and gradually approaches the

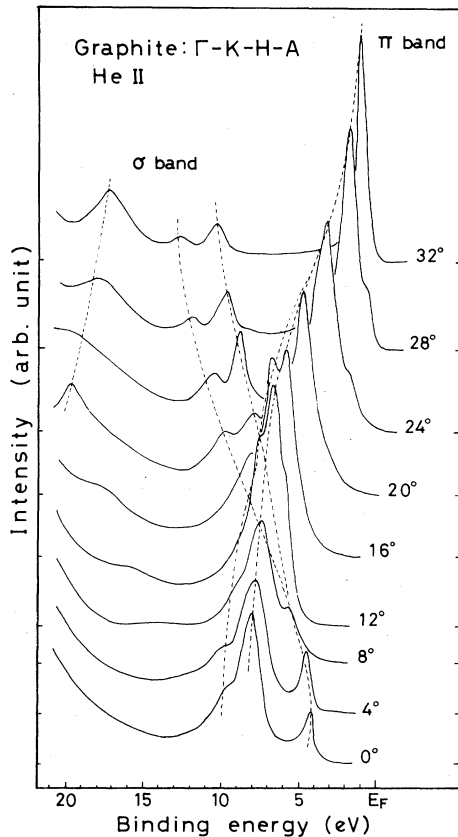


FIG. 3. Angle-resolved He II (40.8 eV) photoemission spectra of graphite measured for the Γ -K-H-A plane. Polar angles referred to the surface normal are denoted on each spectrum. Approximate positions of the π and σ bands are indicated by dashed lines.

Fermi level as the polar angle increases; the first σ band is located at about 4 eV for $\theta=0^\circ$ and moves to higher binding energy, splitting into two well-resolved peaks; the second σ band appears at about 20 eV in the spectrum for $\theta=20^\circ$ and shifts toward lower binding energy. On the other hand, it is difficult to interpret the He I spectra (Fig. 2) straightforwardly in terms of the π and σ valence bands. Especially, spectra taken at low polar angles look largely disturbed by the conduction states and thus should contain much information about the conduction-band structure of graphite.

In Fig. 4 we plot the binding energies E_B of peaks and shoulders in the two sets of ARUPS spectra versus the wave vector parallel to the surface k_{\parallel} using the formula,²²

$$k_{\parallel} = [2m(\hbar\omega - \phi - E_B)/\hbar^2]^{1/2} \sin\theta, \quad (1)$$

where m is the mass of an electron, $\hbar\omega$ the energy of the exciting light, ϕ the work function of graphite (4.6 eV, determined in this study), and θ the polar angle relative to the surface normal. In Fig. 4, experimental results for the Γ -M-L-A plane are also plotted (spectra not shown). Open circles and crosses in Fig. 4 represent prominent peaks and shoulders or small peaks, respectively.

In Fig. 4(b), we clearly find the well-known valence-band structure of graphite: (1) a pair of π bands are located at about 8–10 eV at the Γ (or A) point, dispersing upward as they approach the K (H) and M (L) points; (2) the highest valence band at the Γ (A) point is the σ band at about 4 eV and it disperses downward, splitting into two bands, and the energy separation of the two bands is apparently larger in the Γ -M-L-A plane than in the Γ -K-H-A plane; (3) another σ band having a large $2s$ character appears at higher binding energy (15–18 eV) and at the K (H) point it meets the former σ band dispersing from

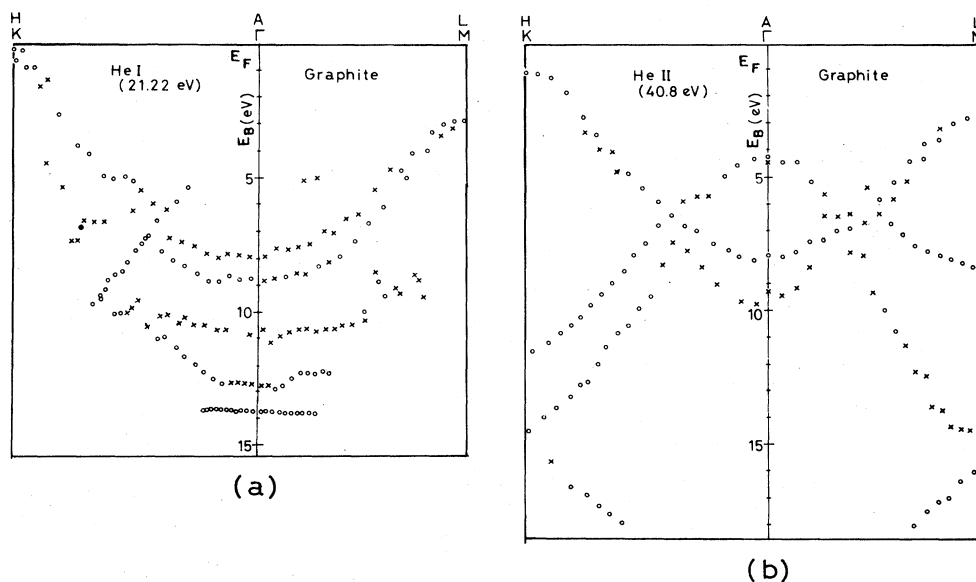


FIG. 4. Binding energies of peaks and shoulders in the photoemission spectra excited by (a) He I and (b) He II resonance lines, plotted against the wave vector parallel to the surface. Circles and crosses indicate prominent and weak features, respectively.

the low binding energy, while at the $M(L)$ point an energy gap of about 1.5 eV opens between the two σ bands. These features agree very well with theoretical calculations^{6,7} of the valence-band structure of graphite. The quantitative comparison of the experimental results from the He II excitation with early experiments¹⁻³ and some three-dimensional band calculations^{6,7,15,16} has been already presented elsewhere.⁵ Nevertheless, it is worthwhile to add a further comment on the valence-band structure of graphite on the energy position of the highest valence σ band at the $\Gamma(A)$ point. Marchand *et al.*⁴ presented very recently their experimental results of an ARUPS study on natural graphite using synchrotron orbital radiation (SOR) of 14–28 eV for the photon energy. They have determined the binding energy of the highest valence σ band at 5.3 eV (Table I in Ref. 4). This value is about 1 eV larger than those of the present (4.3 eV) and other earlier studies (4.6 eV).^{1,2} This difference is beyond experimental error (± 0.1 eV) and cannot be attributed to the interlayer energy dispersion because this σ band is almost flat along the interlayer direction. It is noteworthy that the highest σ band in the present study has a relatively large spectral weight (see Fig. 3) and shows a clear downward dispersion in the vicinity of the $\Gamma(A)$ point [Fig. 4(b)] while the band which Marchand *et al.* have assigned as the highest σ band appears as a very weak structure in their ARUPS spectra and shows almost no energy dispersion (Figs. 1 and 2 in Ref. 4). Therefore, it is most likely that Marchand *et al.* observed an indirect transition or a contribution from conduction states instead of the valence σ band. In the present study with the He I (21.22 eV) excitation, we also could not identify the accurate position of the highest σ band at the $\Gamma(A)$ point; as shown in Figs. 2 and 4(a), the highest σ band looks vague or disappears near the $\Gamma(A)$ point in the He I measurements. The energy of the He I resonance line is closer to the energy range of the SOR study (14–28 eV) than that of the He II line (40.8 eV). We have attributed the absent feature of the highest σ band near the $\Gamma(A)$ point in the He I measurements to the final-state effect; there should be no final states to which electrons are excited from the highest σ band near the $\Gamma(A)$ point by the He I resonance line (21.22 eV). This conjecture is given theoretical support by the band calculation by Tatar and Rabii;⁶ there are no empty states about 18–26 eV above the highest valence σ band at the Γ point (Fig. 6 in Ref. 6).

Next we compare the present experimental results obtained by the two different (He I and He II) exciting energies with each other. As found in Fig. 4, the experimental band structure determined by the He I excitation [Fig. 4(a)] is considerably different from the well-known valence-band structure of graphite, showing a sharp contrast to the result of the He II excitation [Fig. 4(b)]. In the He I measurement, the highest valence σ band does not appear in the vicinity of the $\Gamma(A)$ point and three extra bands appear in the large (above 10 eV) binding energy region and one of them (middle band) shows a remarkable energy dispersion. These three bands are indicated by tick marks in Fig. 2.

The absent feature of the highest σ band at the $\Gamma(A)$ point in the He I measurement as described above is due

to the final state effect. The extra peaks in the He I measurement may represent the conduction bands of graphite because there are no theoretical valence bands which directly correspond to these extra features. The possibility of plasmon loss as an origin of these extra peaks is ruled out by the experimental fact that no structures are found in the same binding-energy region of the He II measurement [Fig. 4(b)]. The plasmon-decay process^{23,24} is also excluded from possible excitation mechanisms for these extra peaks because the π - π plasmon [6.5 eV (Ref. 14)] in graphite does not have sufficient energy to excite these extra peaks about 10 eV above the Fermi level and the other σ - σ plasmon [about 27 eV (Ref. 14)] in graphite cannot be excited by the He I (21.22 eV) resonance line. In order to obtain further experimental confirmation, we performed ARUPS measurements with the Ne I resonance line (16.85 eV) and found that three bands corresponding to the three extra bands in Fig. 4(a) also appear in the Ne I spectra, having nearly the same kinetic energies as in the He I measurement, although the middle band in the Ne I spectra was accidentally superposed with the valence π band. Similar extra features probably due to the conduction states have been already reported in the early ARUPS studies on graphite;^{3,4} Law *et al.*³ found three extra bands in their He I spectra although all of them were almost dispersionless in contrast to the present result, and Marchand *et al.*⁴ also found a stationary peak in their ARUPS spectra having kinetic energy independent of the photon energy. This stationary peak may correspond to the flat band at about 13.8 eV in Fig. 4(a).

In Fig. 5(a), we replot only the experimental points which have no direct correspondence to the valence-band structure determined by the He II excitation [Fig. 4(b)]. These points indicated by open circles (\circ) in Fig. 5(a) are supposed to relate to the conduction states. The vertical energy scale is readjusted to the energy relative to the Fermi level. The experimental results of the angle-resolved secondary electron spectroscopy performed by Law *et al.*³ indicated by crosses ($+$) and the angle-resolved inverse photoelectron spectroscopy by Fauster *et al.*¹³ (\square) are also included in Fig. 5(a) for comparison. Figure 5(b) shows the theoretical conduction-band structure calculated by Holzwarth *et al.*⁷ with the Hedin-Lundqvist potential.

Before we proceed to detailed discussion of the conduction band of graphite, we must comment on the discrepancy between the present and earlier³ ARUPS studies; both of the two studies used the same exciting energy, He I (21.22 eV). Law *et al.*³ found three conduction bands in the energy range similar to that of the present study. However, all of the three bands which they reported were almost dispersionless in the ΓK or ΓM direction (Fig. 3 in Ref. 3) while in this study the middle band shows a remarkable energy dispersion. This discrepancy may arise from the differences in the quality of samples and/or in the resolutions of the ARUPS measurements. Since we do not have sufficient data to discuss the quality of the samples, we will make a short comment on the resolutions in the measurements. The resolutions in this study (ΔE = about 0.1 eV, $\Delta\theta \leq \pm 0.8^\circ$) are about twice as good as those in the early measurements of Law *et al.*

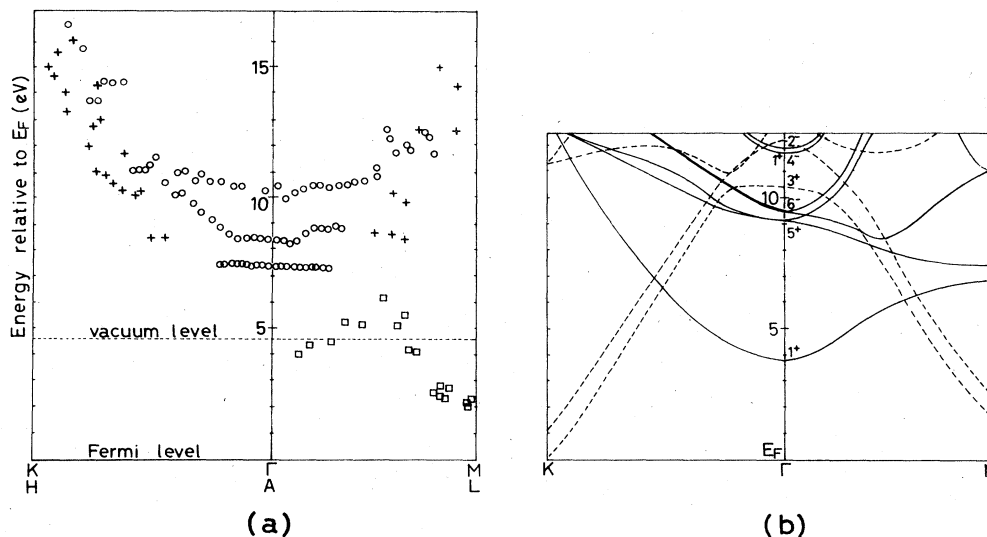


FIG. 5. Comparison of the conduction-band structure determined by experiment and by calculation. (a) Experimental conduction-band structure obtained by the angle-resolved secondary photoelectron spectroscopy (\circ). Experimental results using angle-resolved secondary electron spectroscopy (Ref. 3) ($+$) and angle-resolved inverse photoelectron spectroscopy (Ref. 13) (\square) are also included in this figure. (b) Theoretical conduction-band structure calculated by Holzwarth *et al.* (Ref. 7) with Hedin-Lundqvist potential.

($\Delta E=0.2$ eV, $\Delta\theta=\pm 2^\circ$). The high angular feature of this study is found in the lowest flat band at 7.4 eV in Fig. 5(a); this flat band extends about 1 \AA^{-1} from the $\Gamma(A)$ point in the early experiment by Law *et al.* (Fig. 3 in Ref. 3) while it reaches at most 0.4 \AA^{-1} from the center of the Brillouin zone in this study. They assigned this flat band as the minimum point of the σ^* band at the $\Gamma(A)$ point and attributed the deviation of the experimental points by about 0.5 \AA^{-1} from the theoretical curve to the momentum broadening in the final states, estimating the mean free path of electrons on the flat band as about 5 Å, which is much shorter than the value expected from the universal curve of mean free path versus energy.²⁵ However, the present experimental points are almost on the theoretical curve when we assume a momentum broadening of about 0.1 \AA^{-1} which corresponds to a mean free path of a few tens of angstroms; this value is within the universal curve. Thus, the discrepancy between the present and early³ ARUPS studies may be ascribed to the difference in the energy and angular resolutions; Law *et al.*³ might have overlooked the energy dispersion of the middle band because this band is far broader than the lowest flat band so that it may be missed when the background of secondaries is large and the resolution of a spectrometer is low. As found in Fig. 5(a), the middle dispersive band shows a smooth connection to the experimental results of angle-resolved secondary electron spectroscopy on graphite³ (indicated by $+$) near the center of ΓK (AH). This gives an additional support to the validity of the present measurement.

When we compare the experimental results in Fig. 5(a) with the theoretical band structure⁷ in Fig. 5(b), we find that the overall features of the two are in fair agreement. Fauster *et al.*¹³ have already found experimentally the lowest conduction band at the Γ point by angle-resolved

inverse photoemission spectroscopy; the bottom of the conduction σ band is at about 4.0 eV above the Fermi level as shown in Fig. 5(a). They also found a conduction π band which shows an upward energy dispersion from the M point. These experimental results are in excellent agreement with the band calculation by Holtzwarth *et al.* in Fig. 5(b). These bands, however, are not accessible by photoelectron spectroscopy because major parts of these bands are below the vacuum level.

In light of the experimental fact that the lowest conduction band at the Γ point is below the vacuum level,¹³ we assign the flat band at about 7.4 eV in Fig. 5(a) as the flat part of the σ bands near the Γ_3^+ point at 9.2 eV in Fig. 5(b). As shown in Fig. 2, this band is very narrow (full width at half maximum is about 0.35 eV), reflecting the flat feature of the band and a resulting long lifetime of electrons. This flat band, however, disappears near $\frac{1}{4}\Gamma K$ (AH) in the experiment although the corresponding theoretical σ bands show remarkable upward dispersion near $\frac{1}{4}\Gamma K$. Similar discrepancy is also found for the $\Gamma ML A$ plane. The discontinuity of the experimental flat band may be explained as follows; if the two σ bands degenerate at the Γ_3^+ point disperse almost horizontally to about $\frac{1}{4}\Gamma K$ and there split into two well-separated bands and/or disperse [these features are actually found in the calculation in Fig. 5(b)], these σ bands may become vague or missing in the ARUPS spectra at high polar angles because the peak of these σ bands becomes broad owing to the split into two bands and/or the large lifetime broadening due to the steep dispersion so that these σ bands may be hidden in the large background of secondaries. A similar situation may happen in the $\Gamma ML A$ plane.

The position of this high density of states observed at 7.4 eV above the Fermi level is in good agreement with the position determined in early experiments using angle-

TABLE I. Comparison of energy levels of high density of conduction states observed by several experimental techniques. Energy (in eV) is measured from the Fermi level. Characters (π or σ) of each level assigned by each author are indicated in parentheses.

Present study ^a	UPS		SES		EELS		PYS		IPES		
	Law <i>et al.</i> ^b	Marchand <i>et al.</i> ^c	Hague ^d	Krieg <i>et al.</i> ^e	Willis <i>et al.</i> ^f	Papagno <i>et al.</i> ^g	Hague ^h	Dose <i>et al.</i> ⁱ	Fauster <i>et al.</i> ^j	Baer ^k	Hague ^l
					1.7(π)	1.7(π)		1.7(π)	2.2(π)	2.2(π)	3
7.4(σ)	7.6	7.6(σ)	7.5(σ)	7.6(σ)	7.7(σ)	7.8(σ)		3.4(π)	3.6		
8.4(σ)	8.3	8.2			8.7(σ)				4.0(σ)		
10.0(σ)	10.6	8.6									
		9.5									
		10.1			12.2(π)				9.7(σ)	9.7	9.7(σ)
										14	14.0(σ)

^aAngle-resolved ultraviolet photoelectron spectroscopy (ARUPS) with Kish graphite.

^bReference 3, ARUPS with natural graphite.

^cReference 4, ARUPS with natural graphite.

^dReference 11, photoemission of constant-initial-state mode with HOPG.

^eReference 9, secondary electron spectroscopy (SES) with HOPG.

^fReference 8, SES with HOPG.

^gReference 14, electron-energy-loss spectroscopy (EELS) with HOPG.

^hReference 11, photoyield spectroscopy (PYS) with HOPG.

ⁱReference 12, ultraviolet inverse photoemission spectroscopy (IPES) with carbon film on Pt(111) surface.

^jReference 13, angle-resolved ultraviolet IPES with natural graphite.

^kReference 10, x-ray IPES with HOPG.

^lReference 11, x-ray IPES with HOPG.

integrated secondary electron spectroscopy^{8,9} (7.6–7.7 eV), electron-energy-loss spectroscopy (7.8 eV),¹⁴ angle-integrated photoelectron spectroscopy in the constant-initial-state model¹¹ (7.5 eV), and angle-resolved photoelectron spectroscopy^{3,4} (7.6 eV). Table I summarizes the energy positions of prominent spectral features observed in various spectroscopic studies of the conduction band of graphite. Characters of the experimental bands (π or σ) are also shown in parentheses as each author assigned them. As found in Table I, the calculated Γ_5^+ point in Fig. 5(b) is about 1.6 eV higher than the experiments. Here it is worthwhile to add a comment on this high density of conduction states assigned as Γ_5^+ ; this high density of states at about 7.5 eV above the Fermi level has not yet been observed by any of the ultraviolet^{12,13} or x-ray^{10,11} inverse photoemission studies reported so far (see Table I). The origin of this discrepancy between the inverse photoemission and the other experiments may be inherent in the spectroscopic mechanisms. The discrepancy between inverse photoemission and secondary electron emission has also been pointed out by Law *et al.*;²⁶ they asserted in their recent constant final state spectroscopy on graphite that the “interlayer state” corresponding to the lowest conduction band should be above the vacuum level in contrast to the experimental observation in the inverse photoemission experiment by Fauster *et al.*¹³ Law *et al.* discussed some possible causes for the discrepancy and tentatively attributed it to the fact that inverse photoemission measures the energy difference between the two excited states of the system while secondary-electron emission reflects quasiequilibrium distribution of excitations. The actual origin of the discrepancy, however, is unknown at the present stage and must wait for future studies.

The middle band in Fig. 5(a) is assigned to a pair of σ bands which pass through the Γ_6^- point. This experimental band shows a remarkable energy dispersion in the $\Gamma K H A$ plane and connects smoothly to the experimental points from angle-resolved secondary electron spectroscopy³ (indicated by +) at about $\frac{1}{2}\Gamma K$. The corresponding theoretical σ bands are almost degenerate in the ΓK direction [see Fig. 5(b)] and consequently have a large density of states. This is the main reason why these bands appear as a prominent peak in the ARUPS spectra whereas they have a relatively steep energy dispersion and a resulting rather short lifetime of electrons. The electron lifetime τ in this experimental band estimated from the bandwidth (about 1.3 eV, see Fig. 2) using the uncertainty principle $\Delta E \Delta t \approx h$ is about 3×10^{-15} sec, and the mean free path l calculated with the lifetime and the group velocity (slope of the experimental band) using the formula $l \approx \tau |\partial E / \partial k| / \hbar$ is about 20 Å, which is in good agreement with that for about 10-eV electrons in the universal curve.²⁵ The energy position of the middle band at the $\Gamma(A)$ point is about 8.4 eV above the Fermi level, showing a good agreement with those determined from previous ARUPS studies^{3,4} (8.2–8.6 eV) and a SES study [8.7 eV (Ref. 8)] (see Table I). Therefore, the calculation by Holzwarth *et al.*⁷ [Fig. 5(b)] may overestimate the energy of the Γ_6^- point by about 1 eV. However, we must remark again an inconsistency on this band between the

photoelectron and secondary electron spectroscopies and the inverse photoemission spectroscopies; as shown in Table I there are no structures at 8–9 eV in the inverse photoemission spectra. In fact, Fauster *et al.*¹³ found a prominent peak at about 9.7 eV above the Fermi level (see Table I) in their inverse photoemission spectra and have assigned it as the Γ_6^- point.

The highest experimental band which shows a slight energy dispersion may be assigned to the two σ bands which pass through the Γ_1^+ and Γ_4^- points because both the experimental and theoretical bands show similar dispersing features. If this is the case, an overestimation of the energy level by the calculation⁷ is also found for these Γ_1^+ and Γ_4^- points. This experimental band appearing at about 10 eV at a high-symmetry point in the photoemission spectra (see Table I) may correspond to a remarkable feature at 9.5–9.7 eV in the inverse photoemission spectra, although the spectral feature differs considerably between the two; the inverse photoemission band is pronounced while the photoemission band is relatively weak.

Finally, we should make some comments on the usefulness and development of angle-resolved secondary photoelectron spectroscopy (ARSPEs). As demonstrated in the present study of graphite, photoemission peaks originating in conduction states (conduction peaks) do show remarkable energy dispersions in the angle-resolved photoemission measurements as well as do those of valence states (valence peaks). We believe that this ARSPEs can be applicable to other materials whereas the present case might be special because graphite has a very simple electronic structure. However, ARSPEs has some disadvantages: (1) the electronic states between the Fermi level and vacuum level are not accessible by ARSPEs and angle-resolved inverse photoelectron spectroscopy seems the only experimental technique at present stage to study the energy dispersion of these empty states; (2) both valence and conduction states contribute simultaneously to a photoelectron spectrum so that we must use at least two different exciting photons to separate conduction peaks from valence peaks, and (3) structures due to conduction states in photoemission spectra are in general vague because of the short electron lifetime. The second disadvantage will be overcome when we use the energy-tunable synchrotron orbital radiation; we can measure several sets of ARUPS spectra excited by different energy photons and compare them with each other. The simplest way to distinguish conduction peaks from valence peaks in a photoemission spectrum may be to use relatively high-energy photons, for example 40–100 eV. In photoemission spectra excited by such high-energy photons, structures due to valence states are situated in the large kinetic energy region while the conduction band peaks appear at the low kinetic energy. When we use synchrotron orbital radiation, we can select the most appropriate energy photon with which we can separate clearly conduction bands from valence bands and at the same time avoid possible interference from the valence core levels. The third disadvantage, the vague features of conduction bands in photoemission spectra, may be removed by taking the first or second derivatives of the spectra.

IV. CONCLUSION

We have determined experimentally the energy dispersions of some conduction bands of graphite using the angle-resolved photoelectron spectroscopy. We have identified some high-symmetry points in the conduction-band structure and compared the energy positions with those of early experiments as well as with some theoretical calculations. We have demonstrated the usefulness of angle-resolved (secondary) photoelectron spectroscopy to study conduction-band structure of solids.

ACKNOWLEDGMENT

We are very grateful to Dr. Koyama, Toshiba Ceramics Co., and Professor Suematsu, Tsukuba University for supplying the sample of Kish graphite. We also thank Dr. Suzuki for his collaboration in constructing the highly-angle-resolved photoelectron spectrometer. This work was partially supported by a grant from the Ministry of Education, Japan.

*Present address: Central Research Lab., Idemitsu Kosan Co., Kimitsu, Chiba 292-01, Japan.

- ¹P. M. Williams, *Nuovo Cimento* **38B**, 216 (1977).
- ²W. Eberhardt, I. T. McGovern, E. W. Plummer, and J. E. Fisher, *Phys. Rev. Lett.* **21**, 200 (1980).
- ³A. R. Law, J. J. Barry, and H. P. Hughes, *Phys. Rev. B* **28**, 5332 (1983).
- ⁴D. Marchand, C. Fretigny, M. Lagues, F. Batallan, Ch. Simon, I. Rosenman, and R. Pinchaux, *Phys. Rev. B* **30**, 4788 (1984).
- ⁵T. Takahashi, H. Tokailin, and T. Sagawa, *Solid State Commun.* **52**, 765 (1984).
- ⁶R. C. Tatar and S. Rabii, *Phys. Rev. B* **25**, 4126 (1982).
- ⁷N. A. W. Holzwarth, S. G. Louie, and S. Rabii, *Phys. Rev. B* **26**, 5382 (1982).
- ⁸R. F. Willis, B. Feuerbacher, and B. Fitton, *Phys. Lett.* **34A**, 231 (1971).
- ⁹J. Krieg, P. Oelhafen, and H.-J. Güntherodt, *Solid State Commun.* **42**, 831 (1982).
- ¹⁰Y. Baer, *J. Electron Spectrosc. Relat. Phenomen.* **24**, 95 (1981).
- ¹¹C. F. Hague, *Synth. Met.* **8**, 131 (1983).
- ¹²V. Dose, G. Reusing, and H. Scheidt, *Phys. Rev. B* **26**, 984 (1982).
- ¹³Th. Fauster, F. J. Himpsel, J. E. Fisher, and E. W. Plummer, *Phys. Rev. Lett.* **51**, 430 (1983).
- ¹⁴L. Papagno and L. S. Caputi, *Surf. Sci.* **125**, 530 (1983).
- ¹⁵R. F. Willis, B. Fitton, and G. S. Painter, *Phys. Rev. B* **9**, 1926 (1974).
- ¹⁶C. P. Mallett, *J. Phys. C* **14**, L213 (1981).
- ¹⁷A. D. Baer and G. J. Lapeyre, *Phys. Rev. Lett.* **31**, 304 (1973); G. J. Lapeyre, L. Anderson, P. L. Gobby, and J. A. Knapp, *ibid.* **33**, 1290 (1974); R. E. Thomas, A. Shih, and G. A. Haas, *Surf. Sci.* **75**, 239 (1978); L. Ley, M. Cardona, and R. A. Pollak, in *Photoemission in Solids II*, edited by L. Ley and M. Cardona (Springer, Berlin, 1979), p. 79; J. M. McKay and V. E. Henrich, *Phys. Rev. Lett.* **53**, 2343 (1984).
- ¹⁸N. Joshima, M. Koyama, H. Yoshida, S. Matsuo, and H. Nagasaki, in Proceedings of the International Conference on Carbon, Toyohashi, 1982, edited by M. Inagaki (Toyohashi University of Technology, Toyohashi, 1982), p. 523.
- ¹⁹S. Suzuki, K. Furusawa, M. Terasawa, M. Yoshida, and T. Sagawa, Science Report of Tohoku University, Ser. 8, 1, 16 (1980).
- ²⁰T. Takahashi, H. Tokailin, S. Suzuki, T. Sagawa, and I. Shiro-tani, *Phys. Rev. B* **29**, 1105 (1984).
- ²¹H. Tokailin, T. Takahashi, T. Sagawa, and K. Shindo, *Phys. Rev. B* **30**, 1765 (1984).
- ²²N. V. Smith, in *Photoemission in Solids I*, edited by M. Cardona and L. Ley (Springer, Berlin, 1979), p. 237.
- ²³S. Andersson, *Solid State Commun.* **11**, 1401 (1972).
- ²⁴M. S. Chung and T. E. Everhart, *Phys. Rev. B* **15**, 4699 (1977).
- ²⁵H. Ibach, in *Electron Spectroscopy for Surface Analysis*, edited by H. Ibach (Springer, Berlin, 1977), p. 5.
- ²⁶A. R. Law, M. T. Johnson, H. P. Hughes, and H. A. Padmore, *J. Phys. C* **18**, L297 (1985).